



Vapor wall deposition  
in Teflon chambers

X. Zhang et al.

This discussion paper is/has been under review for the journal Atmospheric Chemistry and Physics (ACP). Please refer to the corresponding final paper in ACP if available.

# Vapor wall deposition in Teflon chambers

X. Zhang<sup>1</sup>, R. H Schwantes<sup>1</sup>, R. C McVay<sup>2</sup>, H Lignell<sup>2</sup>, M. M Coggon<sup>2</sup>,  
R. C Flagan<sup>1,2</sup>, and J. H Seinfeld<sup>1,2</sup>

<sup>1</sup>Division of Engineering and Applied Science, California Institute of Technology, Pasadena, CA, USA

<sup>2</sup>Division of Chemistry and Chemical Engineering, California Institute of Technology, Pasadena, CA, USA

Received: 23 September 2014 – Accepted: 6 October 2014 – Published: 24 October 2014

Correspondence to: J. H. Seinfeld (seinfeld@caltech.edu)

Published by Copernicus Publications on behalf of the European Geosciences Union.

Title Page

Abstract

Introduction

Conclusions

References

Tables

Figures



Back

Close

Full Screen / Esc

Printer-friendly Version

Interactive Discussion



## Abstract

Teflon chambers are ubiquitous in studies of atmospheric chemistry. Secondary organic aerosol (SOA) formation can be substantially underestimated owing to deposition of SOA-forming compounds to chamber walls. We present here an experimental protocol to constrain the nature of wall deposition of organic vapors in Teflon chambers. We measured the wall deposition rates of 25 oxidized organic compounds generated from the photooxidation of isoprene, toluene,  $\alpha$ -pinene, and dodecane in two chambers that had been extensively used and in two new unused chambers. We found that the extent of prior use of the chamber did not significantly affect the sorption behavior of the Teflon films. The dominant parameter governing the extent of wall deposition of a compound is its wall accommodation coefficient ( $\alpha_{w,i}$ ), which can be correlated through its volatility ( $C_i^*$ ) with the number of carbons ( $n_C$ ) and oxygens ( $n_O$ ) in the molecule. Among the 25 compounds studied, the maximum wall deposition rate is approached by the most highly oxygenated and least volatile compounds. The extent to which vapor wall deposition impacts measured SOA yields depends on the competition between uptake of organic vapors by suspended particles and chamber walls. Gas-particle equilibrium partitioning is established relatively rapidly in the presence of perfect accommodation of organic vapors onto particles or when a sufficiently large concentration of suspended particles is present. The timescale associated with vapor wall deposition can vary from minutes to hours depending on the value of  $\alpha_{w,i}$ . For volatile and intermediate volatility organic compounds (small  $\alpha_{w,i}$ ), gas-particle partitioning will be dominant for typical particle number concentrations in chamber experiments. For large  $\alpha_{w,i}$ , vapor transport to particles is suppressed by competition with the chamber walls even with perfect particle accommodation.

## Vapor wall deposition in Teflon chambers

X. Zhang et al.

Title Page

Abstract

Introduction

Conclusions

References

Tables

Figures



Back

Close

Full Screen / Esc

Printer-friendly Version

Interactive Discussion



## 1 Introduction

Understanding of the mechanism and extent of secondary organic aerosol (SOA) formation from oxidation of volatile organic compounds (VOCs) has been derived largely from experiments in Teflon chambers. Chamber-measured SOA yields (mass of SOA formed per mass of VOC reacted) have been widely parameterized into regional/global atmospheric models, and chemical mechanisms leading to SOA formation and aging have been derived based on the gas/particle-phase identification of intermediate/semi/low-volatility compounds generated in controlled chamber experiments. An unavoidable consequence of the use of an environmental chamber is interaction of vapors and particles with the chamber walls. It has been recently established that SOA formation can be substantially underestimated due to deposition of SOA-forming vapors to chamber walls rather than growing particles (Zhang et al., 2014a).

Chamber wall-induced decay of organic vapors was reported almost 30 years ago. Grosjean (1985) and McMurry and Grosjean (1985) measured wall deposition rates of several volatile organic compounds in a chamber constructed from fluorinated ethylene propylene (FEP) Teflon film. The lifetime of the VOCs with respect to wall deposition was found generally to exceed  $\sim 15$  h. Loza et al. (2010) found that deposition of the isoprene oxidation product surrogate, 2,3-epoxy-1,4-butanediol (BEPOX), and glyoxal to FEP Teflon chamber walls is reversible on sufficiently long timescales. Reversible gas-wall partitioning of *n*-alkanes, 1-alkenes, 2-alcohols, and 2-ketones was also observed by Matsunaga and Ziemann (2010).

The extent to which vapors and chamber walls interact is reflected by properties such as the affinity of the wall layer for various organic molecules, the degree of reversibility of the vapor-wall partitioning, and the equilibrium solubility of organic vapors on the walls. Organic materials generated in chamber experiments can deposit to form a coating that can act as the primary absorbing medium, or the Teflon film itself could act as the absorbing medium, in a process akin to the sorption of small molecules by organic polymers. While measurement of vapor wall deposition rates for the thousands

ACPD

14, 26765–26802, 2014

### Vapor wall deposition in Teflon chambers

X. Zhang et al.

Title Page

Abstract

Introduction

Conclusions

References

Tables

Figures



Back

Close

Full Screen / Esc

Printer-friendly Version

Interactive Discussion



of organic molecules that are produced from the oxidation of SOA precursor VOCs is not presently possible, empirical expressions that represent the deposition rates of organic vapors as a function of general molecular properties can be potentially formulated. In any event, the physicochemical nature of vapor-wall interactions needs to be understood.

The ultimate goal of characterizing vapor wall deposition in a chamber is to understand its impact on SOA formation and evolution. We present here an experimental protocol to constrain the nature of organic vapor wall deposition in Teflon chambers. We measured wall-induced dark decay rates of 25 intermediate/semi-volatility organic vapors, which span a range of volatilities and oxidation states, in both unused and previously used chambers constructed with FEP Teflon film. A temperature ramping program (298–318 K) was implemented to study the reversibility of vapor-wall partitioning. A model is developed to describe interactions between organic vapors and chamber walls following the theories for particle wall deposition and gas-particle partitioning. We address the following questions in the present study: (1) what is the physicochemical nature of chamber walls? (2) what are the key parameters that characterize the vapor-wall interactions and how can these values be determined? and (3) how can one predict the wall deposition rate of a specific compound based on its molecular properties?

## 2 Vapor wall deposition – model

Vapor molecules in the well-mixed core of a chamber are transported through a boundary layer adjacent to the walls by a combination of molecular and turbulent diffusion. The transport rate depends on both the molecular properties of individual organic compounds, as well as the extent of turbulent mixing in the chamber. As a vapor molecule encounters the chamber walls, the fraction of those encounters that lead to uptake is represented by the accommodation coefficient ( $\alpha_{w,i}$ ). The accommodation coefficient depends, in principle, on the nature of the wall surface as well as chemical composition of the vapor molecule. Species deposited on the walls may re-evaporate, even-

## Vapor wall deposition in Teflon chambers

X. Zhang et al.

Title Page

Abstract

Introduction

Conclusions

References

Tables

Figures



Back

Close

Full Screen / Esc

Printer-friendly Version

Interactive Discussion



## Vapor wall deposition in Teflon chambers

X. Zhang et al.

Title Page

Abstract

Introduction

Conclusions

References

Tables

Figures



Back

Close

Full Screen / Esc

Printer-friendly Version

Interactive Discussion



tually leading to an equilibrium between the gas-phase and the wall. The extent to which deposited organic vapors evaporate from chamber walls can be characterized by a parameter defined as the equivalent absorbing organic mass on the walls ( $C_w$ ) (Matsunaga and Ziemann, 2010). When  $C_w \rightarrow \infty$ , the wall presents essentially an absorbing medium of infinite extent, and vapor wall deposition is ultimately an irreversible process. Note, however, that the concept of an “equivalent absorbing organic mass” does not necessarily imply that an actual layer of organic material exists on the chamber wall. The quantity  $C_w$  can be regarded as characterizing the equilibrium solubility of individual organic molecules in FEP Teflon polymer and, possibly, in other organic materials deposited on the wall. In summary, two key parameters emerge in the description of vapor deposition on chamber walls: the accommodation coefficient of an species  $i$  on Teflon film ( $\alpha_{w,i}$ ) and the equivalent absorbing organic mass on the wall ( $C_w$ ).

A conservation balance on  $\bar{C}_{v,i}$ , the concentration of vapor  $i$  in the well-mixed core of a chamber that is subject only to the deposition process, is given by:

$$\frac{d\bar{C}_{v,i}}{dt} = -k_{w,depo,i}\bar{C}_{v,i} + k_{w,evap,i}\bar{C}_{w,i} \quad (1)$$

where  $k_{w,depo,i}$  ( $s^{-1}$ ) is the deposition rate coefficient to the wall,  $k_{w,evap,i}$  ( $s^{-1}$ ) is the evaporation rate coefficient from the wall, and  $\bar{C}_{w,i}$  is the concentration of vapor  $i$  that has accumulated on the chamber wall. The dynamic behavior of  $\bar{C}_{w,i}$  is described by a corresponding balance:

$$\frac{d\bar{C}_{w,i}}{dt} = -k_{w,evap,i}\bar{C}_{w,i} + k_{w,depo,i}\bar{C}_{v,i} \quad (2)$$

Note that  $\bar{C}_{w,i}$  is assumed to be zero at the onset of vapor  $i$  generation, ultimately reaching equilibrium with  $\bar{C}_{v,i}$ .

## 2.1 Deposition rate coefficient ( $k_{w,depo,i}$ )

For a chamber that is relatively well mixed, transport to the wall occurs by molecular and turbulent diffusion across a thin boundary layer, of thickness  $\delta$ , adjacent to the chamber walls. The flux due to molecular diffusion is given by  $-D_v \nabla C_{v,i}$ , where  $C_{v,i}$  is the local vapor  $i$  concentration in the boundary layer and  $D_v$  is its molecular diffusivity. The turbulent diffusion flux is expressed as  $-D_e \nabla C_{v,i}$ , where  $D_e$  is the eddy diffusivity. One can invoke the Prandtl mixing length expression near a wall,  $D_e = K_e x^2$ , where  $x$  is the distance from the wall, and  $K_e$  is the coefficient of eddy diffusion (Corner and Pendlebury, 1951; Crump and Seinfeld, 1981). Owing to the small value of  $\delta$ , a quasi-steady state condition exists in the boundary layer, and the concentration of vapor  $i$  within the boundary layer,  $0 \leq x \leq \delta$ , is governed by:

$$\frac{d}{dx} \left[ \left( K_e x^2 + D_v \right) \frac{dC_{v,i}}{dx} \right] = 0 \quad (3)$$

Introducing the dimensionless variable  $z$  by setting  $x = (D_v/K_e)^{1/2} z$ , Eq. (3) becomes:

$$(z^2 + 1) \frac{d^2 C_{v,i}}{dz^2} + 2z \frac{dC_{v,i}}{dz} = 0 \quad (4)$$

subject to the boundary conditions,

$$x = 0 (z = 0) \rightarrow C_{v,i} = C_{0,i}$$

$$x = \delta \left( z = (K_e/D_v)^{1/2} \delta \right) \rightarrow C_{v,i} = \bar{C}_{v,i}$$

where  $C_{0,i}$  and  $\bar{C}_{v,i}$  are concentrations of vapor  $i$  at the wall surface and in the well-mixed core of chamber, respectively. Note that the accommodation coefficient for vapors on the wall is likely less than unity and the steady-state concentration is then

Title Page

Abstract

Introduction

Conclusions

References

Tables

Figures

◀

▶

◀

▶

Back

Close

Full Screen / Esc

Printer-friendly Version

Interactive Discussion



nonzero at the chamber wall surface. The solution of Eq. (4) expressed in the original variables is:

$$C_{v,i} = C_{0,i} + (\bar{C}_{v,i} - C_{0,i}) \frac{\tan^{-1} \left[ (K_e/D_v)^{1/2} x \right]}{\tan^{-1} \left[ (K_e/D_v)^{1/2} \delta \right]} \approx C_{0,i} + (\bar{C}_{v,i} - C_{0,i}) \frac{\tan^{-1} \left[ (K_e/D_v)^{1/2} x \right]}{\pi/2} \quad (5)$$

Physically, turbulent diffusion dominates molecular diffusion at the outer edge of the boundary layer, so that  $(K_e/D_v)^{1/2} \delta \gg 1$ . The vapor flux to the wall surface ( $J_{v,i}$ ) is given by:

$$J_{v,i} = D_v \left. \frac{dC_{v,i}}{dx} \right|_{x=0} = \frac{\alpha_{w,i} \bar{v}_i C_{0,i}}{4} \quad (6)$$

where  $\bar{v}_i$  is the species mean thermal speed. Substitution of Eq. (6) into the derivative of Eq. (5) gives:

$$C_{0,i} = \frac{\bar{C}_{v,i}}{\pi \alpha_{w,i} \bar{v}_i / 8 (D_v K_e)^{1/2} + 1} \quad (7)$$

The deposition coefficient of vapor  $i$  per unit volume is therefore:

$$k_{w,depo,i} = \left( \frac{A}{V} \right) \left( \frac{\alpha_{w,i} \bar{v}_i / 4}{\pi \alpha_{w,i} \bar{v}_i / 8 (D_v K_e)^{1/2} + 1} \right) \quad (8)$$

where  $A$  and  $V$  are the surface area and volume of the chamber, respectively.

Title Page

Abstract

Introduction

Conclusions

References

Tables

Figures

◀

▶

◀

▶

Back

Close

Full Screen / Esc

Printer-friendly Version

Interactive Discussion



## 2.2 Evaporation rate coefficient ( $k_{w, \text{evap}, i}$ )

Without loss of generality, vapor wall deposition can be assumed to be reversible. Gas-particle partitioning theory is applied to describe the relationship between the deposition rate coefficient onto the wall ( $k_{w, \text{depo}, i}$ ) and the evaporation rate coefficient from the wall ( $k_{w, \text{evap}, i}$ ). The gas-wall partition coefficient ( $K_{w, i}$ ), which depends on the vapor pressure of species  $i$ , is given by (Matsunaga and Ziemann, 2010):

$$K_{w, i} = \frac{RT}{p_{L, i}^0 \gamma_i \overline{M}_w} \quad (9)$$

where  $p_{L, i}^0$  is the vapor pressure of compound  $i$  as a liquid,  $\gamma_i$  is its activity coefficient in the wall layer on a mole fraction basis,  $R$  is the gas constant,  $T$  is temperature, and  $\overline{M}_w$  is the average molecular weight of the absorbing organic material on the wall. Then  $k_{w, \text{evap}, i}$  is given by:

$$k_{w, \text{evap}, i} = \frac{k_{w, \text{depo}, i}}{K_{w, i} C_w} \quad (10)$$

where  $C_w$  ( $\text{g m}^{-3}$ ) is an assumed equivalent mass of absorbing organic material on the chamber walls (Matsunaga and Ziemann, 2010).  $C_w$  might well represent the accumulation of deposited organic material from previous chamber experiments, or it could reflect the absorption properties of FEP film itself. We will return to the nature of  $C_w$  shortly. Substitution of Eqs. (8) and (10) into Eq. (1) gives the following conservation equation for the change in the concentration of vapor  $i$  in the well-mixed core of the chamber owing to wall deposition:

$$\frac{d\overline{C}_{v, i}}{dt} = \left(\frac{A}{V}\right) \left(\frac{\alpha_{w, i} \overline{v}_i / 4}{\pi \alpha_{w, i} \overline{v}_i / 8 (D_v K_e)^{1/2} + 1}\right) \left(\frac{\overline{C}_{w, i}}{K_{w, i} C_w} - \overline{C}_{v, i}\right) \quad (11)$$

[Title Page](#)[Abstract](#)[Introduction](#)[Conclusions](#)[References](#)[Tables](#)[Figures](#)[◀](#)[▶](#)[◀](#)[▶](#)[Back](#)[Close](#)[Full Screen / Esc](#)[Printer-friendly Version](#)[Interactive Discussion](#)

### 3 Vapor wall deposition – experiment

Experiments were conducted in the Caltech dual 24 m<sup>3</sup> fluorinated ethylene propylene (FEP) Teflon chambers that are suitable for pristine (low-NO) and polluted (high-NO) conditions (Zhang et al., 2013; Fahnstock et al., 2014; Loza et al., 2014). Figure 1 shows a schematic of the experimental protocol used to measure deposition of organic vapors to the chamber walls. Oxidized organic vapors were generated via photooxidation of four parent VOCs, isoprene, toluene,  $\alpha$ -pinene, and dodecane, in the absence of seed aerosol. Once a sufficient amount of oxidized products is formed with none or limited aerosol formation via nucleation, irradiation is ceased, and the ensuing wall-induced dark decay of the array of oxidation products is monitored by chemical ionization mass spectrometry (CIMS). Following this period, the chambers were heated to investigate the extent to which vapor-wall partitioning is reversible. These experiments were carried out in two chambers that had been used in past SOA studies. Two control experiments were also conducted in two unused 24 m<sup>3</sup> Teflon chambers using the same experimental protocol, see Table 1.

Vapor molecules representing SOA products were generated directly via VOC photooxidation, as opposed to the external injection of commercially available chemical standards. In this manner, uncertainty in the initial vapor concentration due to filling and mixing is avoided. In order to generate a spectrum of oxidized compounds characterized by a combination of different carbon numbers and types of functional groups, isoprene, toluene,  $\alpha$ -pinene, and dodecane were chosen as the parent VOCs. Prior to each experiment, the Teflon chambers were flushed with purified dry air for 12 h at 45 °C, then “conditioned” by UV irradiation for 24 h in the presence of 2 ppm H<sub>2</sub>O<sub>2</sub>, followed by purging with purified dry air for ~4 days at 25 °C. Experiments were carried out under conditions in which the peroxy radicals formed from the initial OH reaction with the parent hydrocarbon react either primarily with NO (so-called high-NO) or HO<sub>2</sub> and RO<sub>2</sub> (so-called low-NO). For low-NO conditions, hydrogen peroxide (H<sub>2</sub>O<sub>2</sub>) was used as the OH source by evaporating 120  $\mu$ L of 50 wt% aqueous solution into the

## Vapor wall deposition in Teflon chambers

X. Zhang et al.

[Title Page](#)[Abstract](#)[Introduction](#)[Conclusions](#)[References](#)[Tables](#)[Figures](#)[Back](#)[Close](#)[Full Screen / Esc](#)[Printer-friendly Version](#)[Interactive Discussion](#)

Vapor wall deposition  
in Teflon chambers

X. Zhang et al.

Title Page

Abstract

Introduction

Conclusions

References

Tables

Figures



Back

Close

Full Screen / Esc

Printer-friendly Version

Interactive Discussion



chamber with  $5 \text{ L min}^{-1}$  of purified air for  $\sim 110$  min, resulting in an approximate starting  $\text{H}_2\text{O}_2$  mixing ratio of 2.0 ppm. For high-NO conditions, nitrous acid (HONO) was used as the OH source by dropwise addition of 15 mL of 1 wt%  $\text{NaNO}_2$  into 30 mL of 10 wt%  $\text{H}_2\text{SO}_4$  in a glass bulb and introduced into the chambers with  $5 \text{ L min}^{-1}$  of purified air for  $\sim 40$  min. Ozone formation is substantially limited in the presence of a high concentration of HONO, and  $\text{NO}_3$  formation is negligible. A measured volume of hydrocarbon (isoprene/toluene/ $\alpha$ -pinene/dodecane) was injected via a syringe into a glass bulb, which was connected to the Teflon chamber. Heated  $5 \text{ L min}^{-1}$  of purified air flowed through the glass bulb into the chamber for 20 min, introducing 25–200 ppb of hydrocarbon into the chamber. After  $\sim 60$  min mixing, photooxidation was initiated by irradiating the chamber with black lights with output wavelength ranging from 300 to 400 nm. Over the course of the irradiation period, the maximum particle mass concentration formed via nucleation ranged from 0.3 to  $2 \mu\text{g m}^{-3}$ , corresponding to a particle surface area to chamber wall area ratio of  $< 10^{-5}$ . Under these conditions, the surface area of particles present in the chamber is sufficiently low that partitioning of organic vapors onto particles is negligible. After  $\sim 1$ –7 h of reaction, UV lights were turned off and the decay of oxidation products due to wall deposition was monitored for  $\sim 13$ –16 h at  $25^\circ\text{C}$ . The chamber temperature was then ramped up to  $45^\circ\text{C}$  during the remaining  $\sim 4$ –6 h of the experiment with other conditions held constant.

Gas-phase organic compounds were monitored using a custom-modified Varian 1200 triple-quadrupole CIMS (Crouse et al., 2006; Paulot et al., 2009). In negative-mode operation,  $\text{CF}_3\text{O}^-$  was used as the reagent ion to cluster with analytes [R] with strong fluorine affinity such as hydroperoxide, producing  $[\text{R}\cdot\text{CF}_3\text{O}]^-$  or  $m/z = [M + 85]^-$ , where  $M$  is the molecular weight of the analyte. For more strongly acidic species [X], the transfer product,  $[\text{X}_{[\text{H}]} \cdot \text{HF}]^-$  or  $m/z = [M + 19]^-$ , is formed during ionization. Carboxylic acids tend to have contributions to both the transfer and cluster products, in which case the trace with higher signal-to-noise ratio is considered. Identification of products by CIMS from the photooxidation of isoprene,  $\alpha$ -pinene, and dode-



can be obtained if the initial and equilibrium gas-phase concentrations of vapor  $i$  are known. Because of the lack of availability of authentic chemical standards to determine absolute vapor concentrations, we estimate  $C_w$  via equilibrium partitioning expressions at two different temperatures, e.g., 298 and 318 K:

$$5 \quad \frac{\bar{C}_{w,i@298K}}{\bar{C}_{v,i@298K}} = \frac{\bar{C}_{tot,i} - \bar{C}_{v,i@298K}}{\bar{C}_{v,i@298K}} = K_{w,i@298K} C_w \quad (12)$$

$$10 \quad \frac{\bar{C}_{w,i@318K}}{\bar{C}_{v,i@318K}} = \frac{\bar{C}_{tot,i} - \bar{C}_{v,i@318K}}{\bar{C}_{v,i@318K}} = K_{w,i@318K} C_w \quad (13)$$

where  $\bar{C}_{tot,i}$  is the total initial concentration of vapor  $i$ ,  $\bar{C}_{v,i@298/318K}$  is the gas-phase concentration (as indicated by the normalized CIMS signal with unit “a.u.”) of vapor  $i$  at 298/318 K, and  $K_{w,i@T}$  is the corresponding partitioning coefficient at temperature  $T$ , see Eq. (9). Note that both sides of Eqs. (12) and (13) are unitless, so that  $C_w$  can be calculated directly from the normalized CIMS signals. The estimated  $C_w$  values vary by approximately five orders of magnitude and exhibit a strong dependence on the volatility of the organics, as shown in Table 2 and Fig. 4a. We will address subsequently why the  $C_w$  values span such a wide range. Matsunaga and Ziemann (2010) reported  $C_w$  values ranging from 10 to 24 mg m<sup>-3</sup> for deposition of a series of C<sub>8</sub>–C<sub>13</sub> 2-alcohols and 2-ketones in a FEP Teflon chamber. Their estimated  $C_w$  values are comparable with those derived from dodecane photooxidation products in the current study, e.g., 3.5 mg m<sup>-3</sup> for hydroxyl dodecanone ( $m/z = (-)285$ ) and 2.8 mg m<sup>-3</sup> for dodecanyl hydroperoxide ( $m/z = (-)287$ ), although the organic vapor generation and measurement procedures between these two studies are quite different.

## 5 Vapor sorption into FEP Teflon films

It is instructive to consider possible mechanisms of organic vapor interactions with Teflon films. Dual sorption mechanisms in glassy polymers have been identified: ordinary dissolution and microvoid-filling (Meares, 1954; Paul, 1979; Paterson et al., 1999; Tsujita, 2003; Kanehashi and Nagai, 2005). From the point of view of solubility behavior, organic polymers such as FEP Teflon may be idealized as high molecular weight organic liquids (Vieth et al., 1966). The polymer rubbery state is hypothesized to represent a thermodynamic equilibrium liquid state within which gas solubility obeys Henry's law. The glassy state, on the other hand, is considered to comprise two components: a hypothetical liquid state and a solid state, the latter containing a distribution of microvoids/holes that act to immobilize a portion of the penetrant molecules when the polymer is below its glass transition temperature ( $T_g = 339\text{K}$  for FEP, Kim and Smith, 1990). The overall solubility of a gas molecule in a glassy polymer has been expressed by (Barrer et al., 1958; Michaels et al., 1963; Vieth et al., 1966; Kanehashi and Nagai, 2005):

$$C = C_D + C_H = k_D + \frac{C'_H bp}{1 + bp} \quad (14)$$

where  $C$  is the total vapor concentration in the glassy polymer,  $C_D$  is the concentration based on Henry's law dissolution,  $C_H$  is the concentration based on Langmuir sorption,  $k_D$  is the Henry's law constant,  $p$  is the partial pressure in the gas phase,  $C'_H$  is the hole saturation constant, and  $b$  is the hole affinity constant. If  $bp \ll 1$ , Eq. (14) reduces to:

$$C = (k_D + C'_H b)p \quad (15)$$

The condition of  $bp \ll 1$  holds in the present situation because the partial pressures of organic vapors generated in the chamber are  $< 10^{-7}$  atm, and the derived hole affinity constants for small organic molecules are  $< 1 \text{ atm}^{-1}$  in glassy polymers (Vieth et al.,

Title Page

Abstract

Introduction

Conclusions

References

Tables

Figures

◀

▶

◀

▶

Back

Close

Full Screen / Esc

Printer-friendly Version

Interactive Discussion



1966; Sada et al., 1988; Kanehashi and Nagai, 2005). If Eq. (15) holds for the equilibrium sorption behavior of organic vapors by FEP films, then the dimensionless form of the effective Henry's law constant ( $H$ ) can be expressed as a function of the partitioning coefficient of vapor  $i$  ( $K_{w,i}$ ) and total absorbing organic mass on chamber walls ( $C_w$ ):

$$H = \frac{\bar{C}_{w,i}}{\bar{C}_{v,i}} = K_{w,i} C_w \alpha (k_D + C'_H b) \quad (16)$$

As shown in Fig. 4b, the derived Henry's law constants ( $H$ ) for the organic oxidation products span approximately two orders of magnitude and depend inversely on saturation concentrations ( $C_i^* / \mu\text{g m}^{-3}$ ). This behavior suggests that organic vapor solubility in FEP films increases with increasing molecular weight, i.e., increasing carbon number and functionalization. This behavior provides a qualitative explanation for the wide range of  $C_w$  values calculated for the 25 organic vapors studied here. Although the solubility of low volatility vapors in the FEP Teflon film is relatively high (large  $H$ ), the total equivalent absorbing organic mass on the walls required for gas-wall partitioning can still be low (small  $C_w$ ) because low volatility compounds tend to partition preferentially in the wall phase (large  $K_{w,i}$ ). As illustrated in Fig. 4b, the dimensionless Henry's law constant of  $m/z = (-)303$ , a product from  $\alpha$ -pinene low-NO photochemistry, is  $\sim 20$  times larger than that of  $m/z = (-)185$ , a product from isoprene +OH under high-NO conditions. The vapor pressure of  $m/z = (-)303$ , however, is  $\sim$  six orders of magnitude lower than that of  $m/z = (-)185$ . As a result, the  $C_w$  value for  $m/z = (-)303$  is  $\sim$  five orders of magnitude smaller than that for  $m/z = (-)185$ . One infers that the equivalent absorbing organic mass on chamber walls derived earlier is not constant but specific to individual organic compounds, i.e., a function of volatility and solubility in FEP Teflon polymer.

Vapor wall deposition  
in Teflon chambers

X. Zhang et al.

Title Page

Abstract

Introduction

Conclusions

References

Tables

Figures

◀

▶

◀

▶

Back

Close

Full Screen / Esc

Printer-friendly Version

Interactive Discussion



## 6 Accommodation coefficient on chamber walls ( $\alpha_{w,i}$ )

One key parameter that emerges from the theory of vapor wall deposition, the total equivalent absorbing organic mass ( $C_w$ ), can be calculated based on equilibrium gas-wall partitioning at two different temperatures. From this information, we can estimate the other key parameter, the accommodation coefficient ( $\alpha_{w,i}$ ), by optimal fitting of the solution of Eq. (11) to CIMS measured organic vapor decay at 298 K:

$$\frac{d\bar{C}_{v,i}}{dt} = \left(\frac{A}{V}\right) \left(\frac{\alpha_{w,i}\bar{v}_i/4}{\pi\alpha_{w,i}\bar{v}_i/8(D_vK_e)^{1/2} + 1}\right) \left(\frac{\bar{C}_{tot,i} - \bar{C}_{v,i}}{K_{w,i}C_w} - \bar{C}_{v,i}\right) \quad (17)$$

Note that Eq. (17) is simply Eq. (11) in which  $\bar{C}_{w,i}$  has been replaced with  $(\bar{C}_{tot,i} - \bar{C}_{v,i})$ . Thus, Eq. (17) constitutes a linear ODE system with one unknown (estimable) parameter. The Levenberg-Marquardt method implemented in MATLAB's "System Identification Toolbox" was used for the nonlinear minimization at each time step of its solution. The best-fit  $\alpha_{w,i}$  value obtained was then substituted into Eq. (17) to give the simulated temporal profile of the organic vapor  $i$  (SIM.1), as shown in Fig. S2 in the Supplement.

The second simulation was carried out by introducing a parameter  $R_{w/v,i} (= \bar{C}_{w,i}/\bar{C}_{v,i})$ , with lower and upper limits of 0 and  $K_{i@298K}C_w$ , respectively.  $R_{w/v,i}$  is a function of time over the course of an experiment. Here we estimate the average value of  $R_{w/v,i}$  for each species  $i$  from the onset of vapor wall deposition to the time when gas-wall equilibrium is reached. Both  $\alpha_{w,i}$  and  $R_{w/v,i}$  are estimated simultaneously via optimal fitting of the solution of the differential equation of  $\bar{C}_{v,i}(t)$  to the observed vapor decay rate:

$$\frac{d\bar{C}_{v,i}}{dt} = \left(\frac{A}{V}\right) \left(\frac{\alpha_{w,i}\bar{v}_i/4}{\pi\alpha_{w,i}\bar{v}_i/8(D_vK_e)^{1/2} + 1}\right) \left(\frac{R_{w/v,i}}{K_{w,i}C_w} - 1\right) \bar{C}_{v,i} \quad (18)$$



Vapor wall deposition  
in Teflon chambers

X. Zhang et al.

Title Page

Abstract

Introduction

Conclusions

References

Tables

Figures



Back

Close

Full Screen / Esc

Printer-friendly Version

Interactive Discussion



vapors. We obtain the somewhat unexpected result that the vapor wall deposition of individual compounds can be adequately parameterized through the accommodation coefficient  $\alpha_{w,i}$  as the single dominant variable. As shown in Table 2 and Fig. 5, estimated values of  $\alpha_{w,i}$  span approximately two orders of magnitude ( $10^{-8}$ – $10^{-6}$ ) and depend inversely on volatility, implying that more highly functionalized compounds dissolve more easily in FEP Teflon films. The correlation of  $\alpha_{w,i}$  with the average carbon oxidation state ( $OS_C$ ), however, is not strong due to the fact that vapor pressures of small molecules, although highly oxidized, are not necessarily low owing to the short carbon backbone.

## 7 Characterizing chamber vapor wall deposition rate

The wall-induced deposition of the 25 organic compounds investigated in the present study can be sufficiently represented by a single parameter, the wall accommodation coefficient ( $\alpha_{w,i}$ ), which is observed to exhibit a strong inverse dependence on  $C_i^*$  (Fig. 5). It is possible to formulate an empirical expression for  $\alpha_{w,i}$  as a function of  $C_i^*$ , a parameter that can be estimated by vapor pressure prediction models.

Linear regression was performed on  $\log_{10} \alpha_{w,i}$  vs.  $\log_{10} C_i^*$  for the 25 organic vapors studied:

$$\log_{10} \alpha_{w,i} = -0.1919 \times \log_{10} C_i^* - 6.32 \quad (20)$$

We employ a group-contribution expression for  $\log_{10} C_i^*$  as a function of carbon number ( $n_C^i$ ) and oxygen number ( $n_O^i$ ) developed by Donahue et al. (2011):

$$\log_{10} C_i^* = \left( n_C^0 - n_C^i \right) b_C - n_O^i b_O - 2 \frac{n_C^i n_O^i}{n_C^i + n_O^i} b_{CO} \quad (21)$$

where  $n_C^0$  is the carbon number of  $1 \mu\text{g m}^{-3}$  alkane ( $n_C^0 \approx 25$ ),  $b_C$  is the carbon-carbon interaction term ( $b_C \approx 0.475$ ),  $b_O$  is the oxygen-oxygen interaction term ( $b_O \approx 2.3$ ), and



partitioning following a small perturbation is given by (Seinfeld and Pandis, 2006):

$$\tau_{g/p,i} = (2\pi N_p \bar{D}_p D_v f(Kn, \alpha_{p,i}))^{-1} \quad (24)$$

where  $N_p$  is the total number concentration of suspended particles,  $\bar{D}_p$  is the number mean particle diameter,  $\alpha_{p,i}$  is the accommodation coefficient of organic vapors on particles,  $Kn = 2\lambda/D_p$  is the Knudsen number, and  $f(Kn, \alpha_{p,i})$  is the correction factor for noncontinuum diffusion and imperfect accommodation. Figure 7 shows the predicted  $\tau_{g/p,i}$  as a function of: (1) the ratio of total particle surface area to chamber wall area ( $R_a$ ) and (2) the accommodation coefficient of organic vapors on particles ( $\alpha_{p,i}$ ). The red solid line represents  $\tau_{g/p,i}$  derived from a typical chamber experiment with seed surface area of  $\sim 1000 \mu\text{m}^2 \text{cm}^{-3}$ . Equilibrium partitioning is established within a few minutes in the presence of perfect accommodation of organic vapors onto particles ( $\alpha_{p,i} = 1$ ) or when a sufficiently large concentration of suspended particles is present (e.g.,  $C_{OA} > 10^5 \mu\text{g m}^{-3}$  when  $\alpha_{p,i} < 10^{-4}$ ).

The timescale associated with vapor wall deposition is given by:

$$\tau_{g/w,i} = k_{w,i}^{-1} \quad (25)$$

The white solid line in Fig. 7 represents the predicted  $\tau_{g/w,i}$ , covering a range of several minutes to several hours, as a function of accommodation coefficient on chamber walls ( $\alpha_{w,i}$ ). The region to the left of the white solid line is that in which  $\tau_{g/w,i}$  and  $\tau_{g/p,i}$  are competitive. For low  $\alpha_{w,i}$  (e.g.,  $< 10^{-8}$ ),  $\tau_{g/w,i}$  is comparable to  $\tau_{g/p,i}$  only if the vapor has a low accommodation coefficient on the particles ( $\alpha_{p,i} < 10^{-4}$ ) or if a small concentration of particles is present in the chamber ( $R_a < 10^{-4}$ ). For  $\alpha_{w,i} > 10^{-4}$ ,  $\tau_{g/w,i}$  is estimated to be of the order of several minutes and, as a result, vapor transport to particles can be suppressed by competition with the chamber walls even with perfect particle accommodation ( $\alpha_{p,i} = 1$ ) or high particle concentrations ( $R_a > 10^{-2}$ ). Overall, a region (confined by the white solid and dash lines in Fig. 7) exists where gas-wall

## Vapor wall deposition in Teflon chambers

X. Zhang et al.

Title Page

Abstract

Introduction

Conclusions

References

Tables

Figures



Back

Close

Full Screen / Esc

Printer-friendly Version

Interactive Discussion



partitioning is competitive with gas-particle partitioning, and in which it is necessary to account for vapor wall deposition when deriving SOA yields from chamber experiments.

## 9 Conclusions

The wall-induced decay of organic vapors is the result of coupled physical processes involving transport of organic vapors from the well-mixed core of a chamber to its walls by molecular and turbulent diffusion, uptake of organic molecules by the Teflon film, and re-evaporation from the walls. The wall-induced dark decay of 25 intermediate/semi-volatility organic compounds generated from the photochemistry of four parent hydrocarbons was observed in the Caltech dual 24 m<sup>3</sup> FEP Teflon chambers. The extent to which organic vapors and chamber walls interact was found to be similar in used vs. unused Teflon chambers. Based on this observation, one concludes that the Teflon film itself acts as an effective sorption medium, and organic materials deposited from past chamber experiments, if they indeed exist, do not significantly impact the sorption behavior of organic molecules. Reversibility in gas-wall partitioning was observed: evaporation of all 25 compounds that had deposited on the walls during an 18 h deposition period occurred when the chamber temperature was increased from 25 to 45 °C.

Based on the model that describes the physical nature of vapor deposition on the chamber walls, it is found that a single parameter, the accommodation coefficient ( $\alpha_{w,i}$ ), governs the extent of the vapor-wall mass transfer process. Moreover,  $\alpha_{w,i}$  exhibits a strong dependence on the molecular properties, such as vapor pressure and oxidation state, of the 25 organics studied. We formulated an empirical expression for  $\alpha_{w,i}$  as a function of the compound vapor pressure, thus affording the possibility to predict the wall deposition rate of intermediate/semi/non-volatility compounds in a Teflon chamber based on their molecular constituency.

Previous studies have observed the chemical transformation of  $\delta$ -hydroxycarbonyls to substituted dihydrofurans on chamber walls (Lim and Ziemann, 2005, 2009; Zhang et al., 2014b), suggesting the potential occurrence of heterogeneous reactions on the

## Vapor wall deposition in Teflon chambers

X. Zhang et al.

Title Page

Abstract

Introduction

Conclusions

References

Tables

Figures



Back

Close

Full Screen / Esc

Printer-friendly Version

Interactive Discussion



chamber wall surface. While the extent to which heterogeneous transformations proceed can be potentially represented through the accommodation coefficient, the occurrence of wall-induced chemistry adds another dimension of complexity in predicting vapor wall deposition rates.

Quantifying the impact of vapor wall deposition on the chamber-derived SOA yield is the next step in assessing the effect of vapor wall deposition of SOA formation and evolution. Future studies will be directed into: (1) experiments to determine the accommodation coefficients of organic vapors on particles for a variety of SOA systems, and (2) state-of-art SOA predictive models that describe the dynamics of vapor-wall and vapor-particle interactions to estimate the fraction of organic vapor fluxes transported to the suspended particles vs. the chamber walls.

**The Supplement related to this article is available online at  
doi:10.5194/acpd-14-26765-2014-supplement.**

*Acknowledgements.* This study was supported by NOAA Climate Program Office's AC4 program, award # NA13OAR4310058 and State of California Air Resources Board agreement 13-321.

## References

- Barrer, R. M., Barrie, J. A., and Slater, J.: Sorption and diffusion in ethyl cellulose. Part II I. Comparison between ethyl cellulose and rubber, *J. Polym. Sci.*, 27, 177–197, 1958.
- Compernelle, S., Ceulemans, K., and Müller, J. F.: EVAPORATION: a new vapour pressure estimation method for organic molecules including non-additivity and intramolecular interactions, *Atmos. Chem. Phys.*, 11, 9431–9450, doi:10.5194/acp-11-9431-2011, 2011.
- Corner, J. and Pendlebury, E. D.: The coagulation and deposition of a stirred aerosol, *P. Phys. Soc. Lond. B.*, 64, 645–654, 1951.

## Vapor wall deposition in Teflon chambers

X. Zhang et al.

Title Page

Abstract

Introduction

Conclusions

References

Tables

Figures



Back

Close

Full Screen / Esc

Printer-friendly Version

Interactive Discussion



Vapor wall deposition  
in Teflon chambers

X. Zhang et al.

Title Page

Abstract

Introduction

Conclusions

References

Tables

Figures



Back

Close

Full Screen / Esc

Printer-friendly Version

Interactive Discussion



- Crouse, J. D., McKinney, K. A., Kwan, A. J., and Wennberg, P. O.: Measurement of gas-phase hydroperoxides by chemical ionization mass spectrometry, *Anal. Chem.*, 78, 6726–6732, 2006.
- Crump, J. G. and Seinfeld, J. H.: Turbulent deposition and gravitational sedimentation of an aerosol in a vessel of arbitrary shape, *J. Aerosol. Sci.*, 12, 405–415, 1981.
- Donahue, N. M., Epstein, S. A., Pandis, S. N., and Robinson, A. L.: A two-dimensional volatility basis set: 1. organic-aerosol mixing thermodynamics, *Atmos. Chem. Phys.*, 11, 3303–3318, doi:10.5194/acp-11-3303-2011, 2011.
- Eddingsaas, N. C., Loza, C. L., Yee, L. D., Seinfeld, J. H., and Wennberg, P. O.:  $\alpha$ -pinene photooxidation under controlled chemical conditions – Part 1: Gas-phase composition in low- and high-NO<sub>x</sub> environments, *Atmos. Chem. Phys.*, 12, 6489–6504, doi:10.5194/acp-12-6489-2012, 2012.
- Fahnestock, K. A. S., Yee, L. D., Loza, C. L., Coggon, M. M., Schwantes, R., Zhang, X., Dalleska, N. F., and Seinfeld, J. H.: Secondary Organic Aerosol Composition from C<sub>12</sub> Alkanes, *J. Phys. Chem. A*, doi:10.1021/jp501779w, 2014.
- Grosjean, D.: Wall loss of gaseous-pollutants in outdoor Teflon chambers, *Environ. Sci. Technol.*, 19, 1059–1065, 1985.
- Kanehashi, S. and Nagai, K.: Analysis of dual-mode model parameters for gas sorption in glassy polymers, *J. Membrane. Sci.*, 253, 117–138, 2005.
- Kim, C. S. and Smith, T. L.: An improved method for measuring the thermal coefficient of linear expansion of flexible polymer-films, *J. Polym. Sci. Pol. Phys.*, 28, 2119–2126, 1990.
- Lim, Y. B. and Ziemann, P. J.: Products and mechanism of secondary organic aerosol formation from reactions of *n*-alkanes with OH radicals in the presence of NO<sub>x</sub>, *Environ. Sci. Technol.*, 39, 9229–9236, 2005.
- Lim, Y. B. and Ziemann, P. J.: Effects of molecular structure on aerosol yields from OH radical-initiated reactions of linear, branched, and cyclic alkanes in the presence of NO<sub>x</sub>, *Environ. Sci. Technol.*, 43, 2328–2334, 2009.
- Loza, C. L., Chan, A. W. H., Galloway, M. M., Keutsch, F. N., Flagan, R. C., and Seinfeld, J. H.: Characterization of vapor wall loss in laboratory chambers, *Environ. Sci. Technol.*, 44, 5074–5078, 2010.
- Loza, C. L., Craven, J. S., Yee, L. D., Coggon, M. M., Schwantes, R. H., Shiraiwa, M., Zhang, X., Schilling, K. A., Ng, N. L., Canagaratna, M. R., Ziemann, P. J., Flagan, R. C., and Seinfeld, J. H.: Secondary organic aerosol formation from *n*-alkanes in the presence of NO<sub>x</sub>, *Environ. Sci. Technol.*, 44, 5074–5078, 2010.

Vapor wall deposition  
in Teflon chambers

X. Zhang et al.

Title Page

Abstract

Introduction

Conclusions

References

Tables

Figures



Back

Close

Full Screen / Esc

Printer-friendly Version

Interactive Discussion



- feld, J. H.: Secondary organic aerosol yields of 12-carbon alkanes, *Atmos. Chem. Phys.*, 14, 1423–1439, doi:10.5194/acp-14-1423-2014, 2014.
- Matsunaga, A. and Ziemann, P. J.: Gas-wall partitioning of organic compounds in a Teflon film chamber and potential effects on reaction product and aerosol yield measurements, *Aerosol Sci. Tech.*, 44, 881–892, 2010.
- McMurry, P. H. and Grosjean, D.: Gas and aerosol wall losses in Teflon film smog chambers, *Environ. Sci. Technol.*, 19, 1176–1182, 1985.
- Meares, P.: The diffusion of gases through polyvinyl acetate, *J. Am. Chem. Soc.*, 76, 3415–3422, 1954.
- Michaels, A. S., Barrie, J. A., and Vieth, W. R.: Solution of gases in polyethylene terephthalate, *J. Appl. Phys.*, 34, 1–13, 1963.
- Pankow, J. F. and Asher, W. E.: SIMPOL.1: a simple group contribution method for predicting vapor pressures and enthalpies of vaporization of multifunctional organic compounds, *Atmos. Chem. Phys.*, 8, 2773–2796, doi:10.5194/acp-8-2773-2008, 2008.
- Paterson, R., Yampol'skii, Y., Fogg, P. G. T., Bokarev, A., Bondar, V., Ilinich, O., and Shishatskii, S.: IUPAC-NIST solubility data series 70. Solubility of gases in glassy polymers, *J. Phys. Chem. Ref. Data*, 28, 1255–1450, 1999.
- Paul, D. R.: Gas sorption and transport in glassy-polymers, *Ber. Bunsen. Phys. Chem.*, 83, 294–302, 1979.
- Paulot, F., Crouse, J. D., Kjaergaard, H. G., Kroll, J. H., Seinfeld, J. H., and Wennberg, P. O.: Isoprene photooxidation: new insights into the production of acids and organic nitrates, *Atmos. Chem. Phys.*, 9, 1479–1501, doi:10.5194/acp-9-1479-2009, 2009.
- Sada, E., Kumazawa, H., Xu, P., and Nishigaki, M.: Mechanism of gas permeation through glassy polymer-films, *J. Membrane Sci.*, 37, 165–179, 1988.
- Seinfeld, J. H. and Pandis, S. N.: *Atmospheric Chemistry and Physics: from Air Pollution to Climate Change*, 2nd edn., John Wiley & Sons, Inc., Hoboken, NJ, 2006.
- Tsujita, Y.: Gas sorption and permeation of glassy polymers with microvoids, *Prog. Polym. Sci.*, 28, 1377–1401, 2003.
- Vieth, W. R., Tam, P. M., and Michaels, A. S.: Dual sorption mechanisms in glassy polystyrene, *J. Colloid. Interf. Sci.*, 22, 360–370, 1966.
- Yee, L. D., Craven, J. S., Loza, C. L., Schilling, K. A., Ng, N. L., Canagaratna, M. R., Ziemann, P. J., Flagan, R. C., and Seinfeld, J. H.: Secondary organic aerosol formation from

low-NO<sub>x</sub> photooxidation of dodecane: Evolution of multigeneration gas-phase chemistry and aerosol composition, *J. Phys. Chem. A.*, 116, 6211–6230, 2012.

Zhang, X. and Seinfeld, J. H.: A functional group oxidation model (FGOM) for SOA formation and aging, *Atmos. Chem. Phys.*, 13, 5907–5926, doi:10.5194/acp-13-5907-2013, 2013.

5 Zhang, X., Cappa, C. D., Jathar, S. H., McVay, R. C., Ensberg, J. J., Kleeman, M. J., and Seinfeld, J. H.: Influence of vapor wall loss in laboratory chambers on yields of secondary organic aerosol, *P. Natl. Acad. Sci. USA*, 111, 5802–5807, 2014a.

Zhang, X., Schwantes, R. H., Coggon, M. M., Loza, C. L., Schilling, K. A., Flagan, R. C., and Seinfeld, J. H.: Role of ozone in SOA formation from alkane photooxidation, *Atmos. Chem. Phys.*, 14, 1733–1753, doi:10.5194/acp-14-1733-2014, 2014b.

10

ACPD

14, 26765–26802, 2014

## Vapor wall deposition in Teflon chambers

X. Zhang et al.

Title Page

Abstract

Introduction

Conclusions

References

Tables

Figures

◀

▶

◀

▶

Back

Close

Full Screen / Esc

Printer-friendly Version

Interactive Discussion



Vapor wall deposition  
in Teflon chambers

X. Zhang et al.

Title Page

Abstract

Introduction

Conclusions

References

Tables

Figures

◀

▶

◀

▶

Back

Close

Full Screen / Esc

Printer-friendly Version

Interactive Discussion

**Table 1.** Experimental conditions for production of oxidized organic vapors.

	Exp.#	Lights on (h)	Lights off (h)	<i>T</i> program <sup>a</sup> (K { h–h})	OH source	VOC	HC (ppb)	(NO) (ppb)	(NO <sub>2</sub> ) (ppb)	Maximum Particle conc. (μg m <sup>-3</sup> )	FEP Bag condition
high-NO	1	~ 1	~ 24.2	298 {0–17.6} 318 {19.9–25.2}	HONO	<i>α</i> -pinene	~ 30	242	458	~ 0.4	Used
	2	~ 1	~ 24.2	298 {0–17.6} 318 {19.9–25.2}	HONO	<i>α</i> -pinene	~ 30	229	371	~ 0.3	Unused
	3	~ 1	~ 23.8	298 {0–17.3} 318 {20.9–24.8}	HONO	dodecane	~ 50	275	556	~ 2.1	Used
	4	~ 2	~ 23	298 {0–17.3} 318 {20.8–25}	HONO	isoprene	~ 200	243	460	~ 0.2	Used
low-NO	5	~ 1	~ 24.2	298 {0–17.8} 318 {20.3–25.2}	H <sub>2</sub> O <sub>2</sub>	<i>α</i> -pinene	~ 30	< DL	< DL	~ 1.2	Used
	6	~ 1	~ 24.2	298 {0–17.8} 318 {20.3–25.2}	H <sub>2</sub> O <sub>2</sub>	<i>α</i> -pinene	~ 30	< DL	< DL	~ 1.1	Unused
	7	~ 7	~ 21.6	298 {0–20.6} 318 {22–28.6}	H <sub>2</sub> O <sub>2</sub>	dodecane	~ 50	< DL	< DL	~ 0.	Used
	8	~ 5	~ 24.7	298 {0–21.3} 318 {24.7–29.7}	H <sub>2</sub> O <sub>2</sub>	toluene	~ 100	< DL	< DL	~ 0.1	Used

<sup>a</sup>The temperature is controlled at 298 K for the first ~ 20 h of the experiment, including ~ 1–7 h irradiation and ~ 13–16 h darkness, and then ramped up to 318 K within ~ 3 h and held for ~ 4–6 h.

Vapor wall deposition  
in Teflon chambers

X. Zhang et al.

**Table 2.** Best-fit values of vapor-wall accommodation coefficient ( $\alpha_{w,i}$ ) and calculated equivalent absorbing organic mass ( $C_w$ ) on chamber walls for vapors with structure proposed based on the CIMS measurement.

Observed $m/z$	Molecular Weight	Chemical Formula	Proposed Structure	Vapor pressure (atm @ 298 K) <sup>a</sup>	Vapor wall deposition rate $k_{w,i}$ (s <sup>-1</sup> ) <sup>b</sup>	$\alpha_{w,i}$ <sup>c</sup>	$C_w$ (g m <sup>-3</sup> ) <sup>d</sup>	Formation Mechanism
269 (-)	184	C <sub>10</sub> H <sub>16</sub> O <sub>3</sub>		$9.64 \times 10^{-8}$	$(8.95 \pm 2.55) \times 10^{-6}$	$(9.15 \pm 2.63) \times 10^{-8}$	$(6.59 \pm 3.43) \times 10^{-4}$	$\alpha$ -pinene + OH (low-NO <sub>x</sub> ) Eddingsaas et al. (2012)
285 (-)	200	C <sub>10</sub> H <sub>16</sub> O <sub>4</sub>		$1.05 \times 10^{-6}$	$(2.98 \pm 1.14) \times 10^{-6}$	$(3.24 \pm 1.20) \times 10^{-8}$	$(5.90 \pm 3.65) \times 10^{-3}$	
253 (-)	168	C <sub>10</sub> H <sub>16</sub> O <sub>2</sub>		$6.79 \times 10^{-6}$	$(4.40 \pm 0.70) \times 10^{-6}$	$(4.31 \pm 0.68) \times 10^{-8}$	$(4.57 \pm 2.45) \times 10^{-3}$	
257 (-)	172	C <sub>9</sub> H <sub>16</sub> O <sub>3</sub>		$2.65 \times 10^{-6}$	$(3.19 \pm 3.13) \times 10^{-6}$	$(3.12 \pm 3.07) \times 10^{-8}$	$(6.31 \pm 4.98) \times 10^{-3}$	
271 (-)	186	C <sub>10</sub> H <sub>18</sub> O <sub>3</sub>		$5.14 \times 10^{-8}$	$(1.09 \pm 0.06) \times 10^{-5}$	$(1.15 \pm 0.07) \times 10^{-7}$	$(5.56 \pm 3.86) \times 10^{-5}$	
303 (-)	218	C <sub>10</sub> H <sub>18</sub> O <sub>5</sub>		$1.56 \times 10^{-10}$	$(1.32 \pm 0.19) \times 10^{-5}$	$(1.49 \pm 0.22) \times 10^{-7}$	$(1.12 \pm 1.19) \times 10^{-6}$	

<sup>a</sup> Vapor pressures are estimated from the average of predictions from the two group contribution methods, "SIMPOL.1" (Pankow and Asher, 2008) and "EVAPORATION" (Compernelle et al., 2011).<sup>b</sup> The vapor wall deposition rate ( $k_{w,i}$ ) is calculated by Eq. (19b).<sup>c</sup> The accommodation coefficient ( $\alpha_{w,i}$ ) is calculated via optimal fitting of the coefficient expression of  $\bar{C}_{v,i}$  in Eq. (19a) to the CIMS measured vapor decay rate assuming first-order kinetics and irreversible gas-wall partitioning.<sup>d</sup>  $C_w$  is calculated from the combination of Eqs. (12) and (13).

Title Page

Abstract

Introduction

Conclusions

References

Tables

Figures

◀

▶

◀

▶

Back

Close

Full Screen / Esc

Printer-friendly Version

Interactive Discussion



Vapor wall deposition  
in Teflon chambers

X. Zhang et al.

Table 2. Continued.

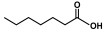
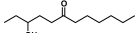
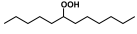
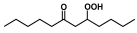
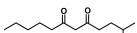
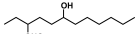
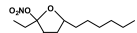
Observed $m/z$	Molecular Weight	Chemical Formula	Proposed Structure	Vapor pressure (atm @ 298 K) <sup>a</sup>	Vapor wall deposition rate $k_{w,i}$ (s <sup>-1</sup> ) <sup>b</sup>	$\alpha_{w,i}$ <sup>c</sup>	$C_w$ (g m <sup>-3</sup> ) <sup>d</sup>	Formation Mechanism
227 (-)	142	C <sub>7</sub> H <sub>10</sub> O <sub>3</sub>		$1.24 \times 10^{-5}$	$(1.63 \pm 0.50) \times 10^{-5}$	$(1.52 \pm 0.15) \times 10^{-7}$	$(1.01 \pm 0.91) \times 10^{-2}$	$\alpha$ -pinene + OH (high-NO <sub>x</sub> ) Eddingsaas et al. (2012)
269 (-)	184	C <sub>10</sub> H <sub>16</sub> O <sub>3</sub>		$3.48 \times 10^{-9}$	$(1.94 \pm 0.30) \times 10^{-5}$	$(1.97 \pm 0.32) \times 10^{-7}$	$(2.80 \pm 1.02) \times 10^{-5}$	
285 (-)	200	C <sub>10</sub> H <sub>16</sub> O <sub>4</sub>		$6.32 \times 10^{-11}$	$(1.51 \pm 0.15) \times 10^{-5}$	$(1.62 \pm 0.16) \times 10^{-7}$	$(3.83 \pm 3.11) \times 10^{-7}$	
300 (-)	215	C <sub>10</sub> H <sub>17</sub> O <sub>4</sub> N		$1.53 \times 10^{-7}$	$(1.19 \pm 0.13) \times 10^{-5}$	$(1.34 \pm 0.14) \times 10^{-7}$	$(1.79 \pm 0.06) \times 10^{-4}$	
314 (-)	229	C <sub>10</sub> H <sub>15</sub> O <sub>5</sub> N		$1.52 \times 10^{-7}$	$(2.31 \pm 0.21) \times 10^{-5}$	$(2.94 \pm 0.26) \times 10^{-7}$	$(1.14 \pm 0.10) \times 10^{-3}$	
316 (-)	231	C <sub>10</sub> H <sub>17</sub> O <sub>5</sub> N		$9.03 \times 10^{-10}$	$(1.85 \pm 0.14) \times 10^{-5}$	$(2.19 \pm 0.17) \times 10^{-7}$	$(5.36 \pm 9.85) \times 10^{-6}$	

<sup>a</sup> Vapor pressures are estimated from the average of predictions from the two group contribution methods, "SIMPOL-1" (Pankow and Asher, 2008) and "EVAPORATION" (Compernelle et al., 2011).<sup>b</sup> The vapor wall deposition rate ( $k_{w,i}$ ) is calculated by Eq. (19b).<sup>c</sup> The accommodation coefficient ( $\alpha_{w,i}$ ) is calculated via optimal fitting of the coefficient expression of  $\bar{C}_{v,i}$  in Eq. (19a) to the CIMS measured vapor decay rate assuming first-order kinetics and irreversible gas-wall partitioning.<sup>d</sup>  $C_w$  is calculated from the combination of Eqs. (12) and (13).

Vapor wall deposition  
in Teflon chambers

X. Zhang et al.

Table 2. Continued.

Observed $m/z$	Molecular Weight	Chemical Formula	Proposed Structure	Vapor pressure (atm @ 298 K) <sup>a</sup>	Vapor wall deposition rate $k_{w,i}$ (s <sup>-1</sup> ) <sup>b</sup>	$\alpha_{w,i}$ <sup>c</sup>	$C_w$ (g m <sup>-3</sup> ) <sup>d</sup>	Formation Mechanism
215 (-)	130	C <sub>7</sub> H <sub>14</sub> O <sub>2</sub>		$1.98 \times 10^{-5}$	$(5.27 \pm 1.74) \times 10^{-6}$	$(4.50 \pm 1.49) \times 10^{-8}$	$(3.10 \pm 0.55) \times 10^{-2}$	Dodecane + OH (low-NO <sub>x</sub> ) Yee et al. (2012)
285 (-)	200	C <sub>12</sub> H <sub>24</sub> O <sub>2</sub>		$3.58 \times 10^{-7}$	$(1.32 \pm 0.44) \times 10^{-5}$	$(1.42 \pm 0.46) \times 10^{-7}$	$(3.50 \pm 0.81) \times 10^{-3}$	
287 (-)	202	C <sub>12</sub> H <sub>26</sub> O <sub>2</sub>		$1.21 \times 10^{-6}$	$(8.25 \pm 0.67) \times 10^{-6}$	$(8.79 \pm 0.73) \times 10^{-8}$	$(2.81 \pm 1.92) \times 10^{-3}$	
301 (-)	216	C <sub>12</sub> H <sub>24</sub> O <sub>3</sub>		$1.30 \times 10^{-7}$	$(1.19 \pm 0.13) \times 10^{-5}$	$(1.35 \pm 0.15) \times 10^{-7}$	$(8.39 \pm 7.24) \times 10^{-4}$	
315 (-)	230	C <sub>12</sub> H <sub>22</sub> O <sub>4</sub>		$1.56 \times 10^{-8}$	$(2.68 \pm 0.49) \times 10^{-5}$	$(3.17 \pm 0.61) \times 10^{-7}$	$(1.79 \pm 2.15) \times 10^{-4}$	
332 (-)	247	C <sub>12</sub> H <sub>25</sub> O <sub>4</sub> N		$2.17 \times 10^{-8}$	$(1.55 \pm 0.07) \times 10^{-5}$	$(1.86 \pm 0.09) \times 10^{-7}$	$(3.93 \pm 0.46) \times 10^{-4}$	Dodecane + OH (high-NO <sub>x</sub> ) Zhang et al. (2012)
346 (-)	261	C <sub>12</sub> H <sub>23</sub> O <sub>5</sub> N		$4.46 \times 10^{-9}$	$(2.33 \pm 0.25) \times 10^{-5}$	$(2.91 \pm 0.33) \times 10^{-7}$	$(1.87 \pm 0.21) \times 10^{-5}$	

<sup>a</sup> Vapor pressures are estimated from the average of predictions from the two group contribution methods, "SIMPOL-1" (Pankov and Asher, 2008) and "EVAPORATION" (Compernelle et al., 2011).<sup>b</sup> The vapor wall deposition rate ( $k_{w,i}$ ) is calculated by Eq. (19b).<sup>c</sup> The accommodation coefficient ( $\alpha_{w,i}$ ) is calculated via optimal fitting of the coefficient expression of  $\bar{C}_{v,i}$  in Eq. (19a) to the CIMS measured vapor decay rate assuming first-order kinetics and irreversible gas-wall partitioning.<sup>d</sup>  $C_w$  is calculated from the combination of Eqs. (12) and (13).

Vapor wall deposition  
in Teflon chambers

X. Zhang et al.

Title Page

Abstract

Introduction

Conclusions

References

Tables

Figures

◀

▶

◀

▶

Back

Close

Full Screen / Esc

Printer-friendly Version

Interactive Discussion



Table 2. Continued.

Observed $m/z$	Molecular Weight	Chemical Formula	Proposed Structure	Vapor pressure (atm @ 298 K) <sup>a</sup>	Vapor wall deposition rate $k_{w,i}$ (s <sup>-1</sup> ) <sup>b</sup>	$\alpha_{w,i}$ <sup>c</sup>	$C_w$ (g m <sup>-3</sup> ) <sup>d</sup>	Formation Mechanism
141 (-)	122	C <sub>7</sub> H <sub>6</sub> O <sub>2</sub>		$5.30 \times 10^{-6}$	$(2.04 \pm 1.88) \times 10^{-6}$	$(1.68 \pm 1.35) \times 10^{-8}$	$(1.13 \pm 0.07) \times 10^{-2}$	toluene + OH (low-NO <sub>x</sub> ) MCM v3.2
209 (-)	124	C <sub>7</sub> H <sub>8</sub> O <sub>2</sub>		$4.89 \times 10^{-5}$	$(5.78 \pm 1.93) \times 10^{-6}$	$(4.82 \pm 1.62) \times 10^{-8}$	$(7.03 \pm 1.42) \times 10^{-2}$	
241 (-)	156	C <sub>7</sub> H <sub>8</sub> O <sub>4</sub>		$4.00 \times 10^{-6}$	$(2.04 \pm 0.40) \times 10^{-5}$	$(1.95 \pm 0.39) \times 10^{-7}$	$(2.66 \pm 0.71) \times 10^{-2}$	
175 (-)	90	C <sub>3</sub> H <sub>6</sub> O <sub>3</sub>		$2.21 \times 10^{-4}$	$(9.68 \pm 1.51) \times 10^{-6}$	$(6.90 \pm 1.08) \times 10^{-8}$	$(3.03 \pm 1.10) \times 10^{-1}$	isoprene + OH (high-NO <sub>x</sub> ) Paulot et al. (2009)
185 (-)	100	C <sub>5</sub> H <sub>8</sub> O <sub>2</sub>		$1.73 \times 10^{-4}$	$(6.58 \pm 0.30) \times 10^{-6}$	$(4.93 \pm 0.22) \times 10^{-8}$	$(7.70 \pm 2.01) \times 10^{-2}$	
199 (-)	114	C <sub>5</sub> H <sub>8</sub> O <sub>3</sub>		$8.17 \times 10^{-6}$	$(2.46 \pm 0.81) \times 10^{-6}$	$(1.96 \pm 0.64) \times 10^{-8}$	$(1.23 \pm 0.31) \times 10^{-2}$	
217 (-)	132	C <sub>5</sub> H <sub>8</sub> O <sub>4</sub>		$2.70 \times 10^{-7}$	$(1.40 \pm 0.11) \times 10^{-5}$	$(1.22 \pm 0.10) \times 10^{-7}$	$(1.15 \pm 0.60) \times 10^{-4}$	
232 (-)	147	C <sub>5</sub> H <sub>9</sub> O <sub>4</sub> N		$2.34 \times 10^{-5}$	$(5.24 \pm 0.24) \times 10^{-6}$	$(4.76 \pm 0.22) \times 10^{-8}$	$(1.78 \pm 0.42) \times 10^{-3}$	
234 (-)	149	C <sub>4</sub> H <sub>7</sub> O <sub>5</sub> N		$3.93 \times 10^{-6}$	$(3.23 \pm 1.30) \times 10^{-6}$	$(2.97 \pm 0.28) \times 10^{-8}$	$(5.16 \pm 1.36) \times 10^{-4}$	
311 (-)	226	C <sub>5</sub> H <sub>10</sub> O <sub>8</sub> N <sub>2</sub>		$1.15 \times 10^{-9}$	$(3.10 \pm 0.45) \times 10^{-5}$	$(3.66 \pm 0.54) \times 10^{-7}$	$(8.27 \pm 1.24) \times 10^{-6}$	

<sup>a</sup> Vapor pressures are estimated from the average of predictions from the two group contribution methods, "SIMPOL-1" (Pankow and Asher, 2008) and "EVAPORATION" (Compernelle et al., 2011).<sup>b</sup> The vapor wall deposition rate ( $k_{w,i}$ ) is calculated by Eq. (19b).<sup>c</sup> The accommodation coefficient ( $\alpha_{w,i}$ ) is calculated via optimal fitting of the coefficient expression of  $\bar{C}_{v,i}$  in Eq. (19a) to the CIMS measured vapor decay rate assuming first-order kinetics and irreversible gas-wall partitioning.<sup>d</sup>  $C_w$  is calculated from the combination of Eqs. (12) and (13).

Vapor wall deposition  
in Teflon chambers

X. Zhang et al.

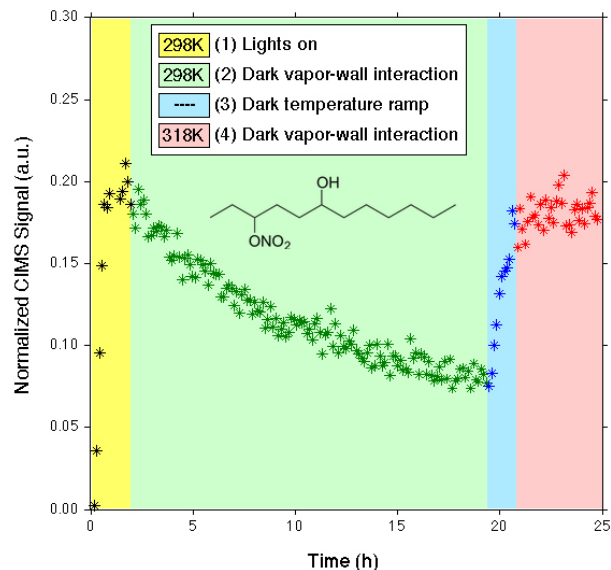


**Figure 1.** Example of the experimental procedure to assess vapor wall deposition using 3-nitroxy-6-dodecanol ( $m/z = (-) 332$ ): Period (1) organic oxidation product generation; Period (2) vapor wall deposition at 298 K in the dark; Period (3) chamber temperature ramp from 298 K to 318 K; and Period (4) temperature held at 318 K in the dark.

[Title Page](#)[Abstract](#)[Introduction](#)[Conclusions](#)[References](#)[Tables](#)[Figures](#)[◀](#)[▶](#)[◀](#)[▶](#)[Back](#)[Close](#)[Full Screen / Esc](#)[Printer-friendly Version](#)[Interactive Discussion](#)

Vapor wall deposition  
in Teflon chambers

X. Zhang et al.

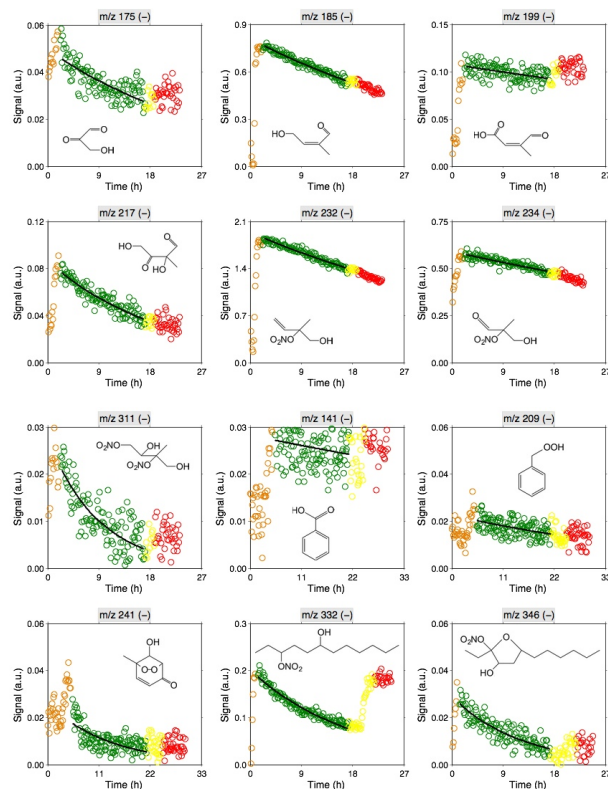


**Figure 2.** CIMS traces of oxidized organic vapors generated from the photooxidation of isoprene, toluene,  $\alpha$ -pinene and dodecane under high/low-NO conditions over the four chamber periods in Fig. 1. Colored circles represent CIMS measured normalized signals during vapor generation (orange), vapor wall deposition at 298 K (green), temperature ramp (yellow), and vapor re-evaporation at 318 K (red). Black lines represent the best-fit first-order decay during the wall deposition period.

Title Page

Abstract

Introduction

Conclusions

References

Tables

Figures



Back

Close

Full Screen / Esc

Printer-friendly Version

Interactive Discussion



Vapor wall deposition  
in Teflon chambers

X. Zhang et al.

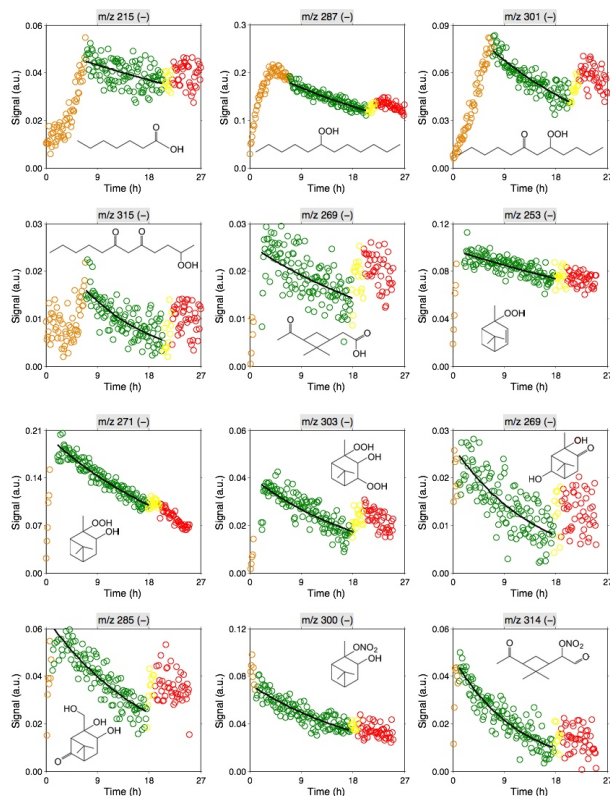


Figure 2. Continued.

Title Page

Abstract

Introduction

Conclusions

References

Tables

Figures



Back

Close

Full Screen / Esc

Printer-friendly Version

Interactive Discussion



Vapor wall deposition  
in Teflon chambers

X. Zhang et al.

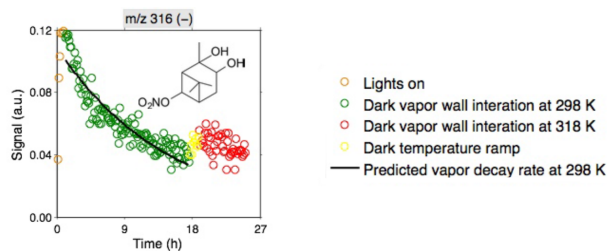


Figure 2. Continued.

Title Page

Abstract

Introduction

Conclusions

References

Tables

Figures

◀

▶

◀

▶

Back

Close

Full Screen / Esc

Printer-friendly Version

Interactive Discussion



Vapor wall deposition  
in Teflon chambers

X. Zhang et al.

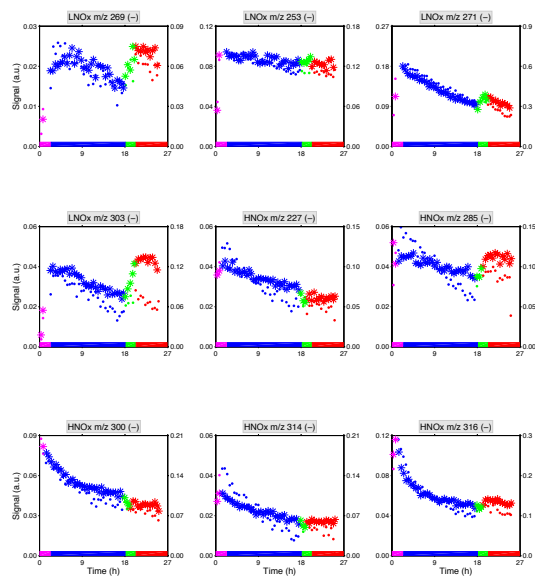


**Figure 3.** Comparison of vapor-wall interactions for  $\alpha$ -pinene+OH products under controlled experimental conditions in used (filled circle) vs. unused (asterisk mark) Teflon chambers. 30 min averaged data are shown here for clarity. Colored bands denote successive experimental periods: vapor generation (magenta), vapor wall deposition at 298 K (blue), temperature ramp (green), and vapor re-evaporation at 318 K (red).

[Title Page](#)[Abstract](#)[Introduction](#)[Conclusions](#)[References](#)[Tables](#)[Figures](#)[Back](#)[Close](#)[Full Screen / Esc](#)[Printer-friendly Version](#)[Interactive Discussion](#)

Vapor wall deposition  
in Teflon chambers

X. Zhang et al.

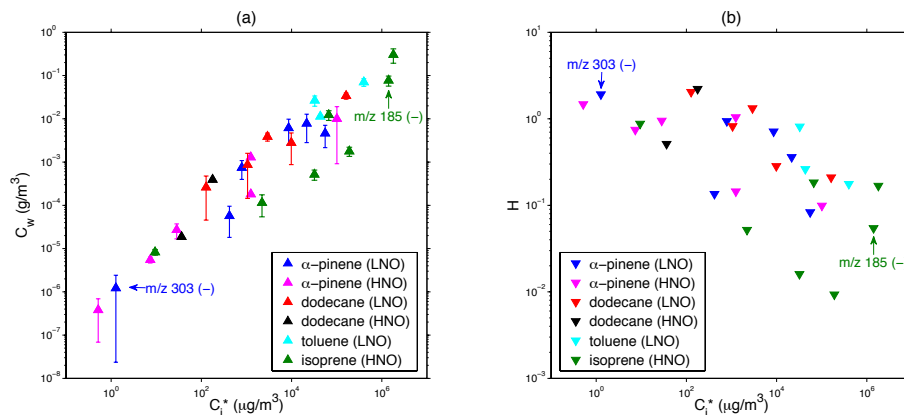


**Figure 4.** Inferred total amount of **(a)** equivalent absorbing organic mass on chamber walls,  $C_w$  (g m<sup>-3</sup>), and **(b)** dimensionless Henry's law constants,  $H$ , as a function of saturation concentration,  $C_i^*$  (μg m<sup>-3</sup>). Estimated vapor pressures of organic compounds studied here are obtained from the average of predictions from the two group contribution methods, “SIMPOL.1” (Pankow and Asher, 2008) and “EVAPORATION” (Compennolle et al., 2011). The uncertainty bars give the upper and lower limits of  $C_w$  values derived from Eq. (9), together with Eqs. (12) and (13), when either “EVAPORATION” or “SIMPOL.1” is used to estimate vapor pressures.

Vapor wall deposition  
in Teflon chambers

X. Zhang et al.

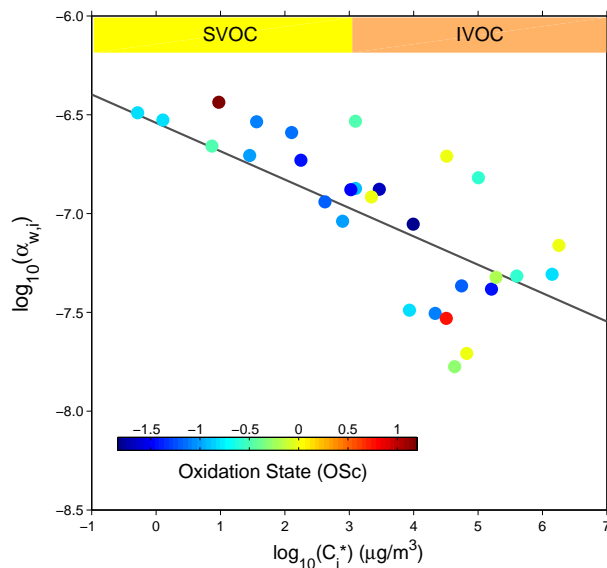


**Figure 5.** Inferred accommodation coefficients of organic oxidation products on chamber walls ( $\log_{10}(\alpha_{w,i})$ ) as a function of saturation concentrations ( $\log_{10}(C_i^*)$ ) and average carbon oxidation state ( $OS_C$ ). Colored filled circles represent the best-fit  $\alpha_w$  assuming irreversible gas-wall partitioning. The black solid line represents the linear regression of  $\log_{10}(\alpha_{w,i})$  vs.  $\log_{10}(C_i^*)$  for all compounds.

[Title Page](#)[Abstract](#)[Introduction](#)[Conclusions](#)[References](#)[Tables](#)[Figures](#)[◀](#)[▶](#)[◀](#)[▶](#)[Back](#)[Close](#)[Full Screen / Esc](#)[Printer-friendly Version](#)[Interactive Discussion](#)

Vapor wall deposition  
in Teflon chambers

X. Zhang et al.

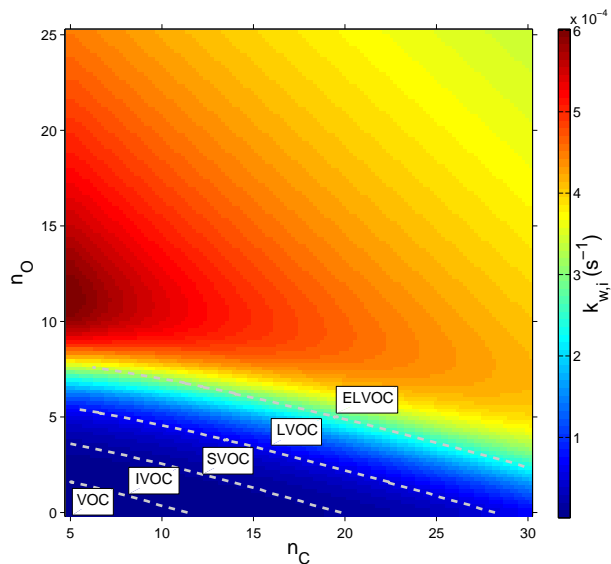


**Figure 6.** Predicted vapor wall deposition rate ( $k_{w,i}/s^{-1}$ ) of organic compounds in a Teflon chamber as a function of carbon number ( $n_C$ ) and oxygen number ( $n_O$ ).

[Title Page](#)[Abstract](#)[Introduction](#)[Conclusions](#)[References](#)[Tables](#)[Figures](#)[◀](#)[▶](#)[◀](#)[▶](#)[Back](#)[Close](#)[Full Screen / Esc](#)[Printer-friendly Version](#)[Interactive Discussion](#)

Vapor wall deposition  
in Teflon chambers

X. Zhang et al.

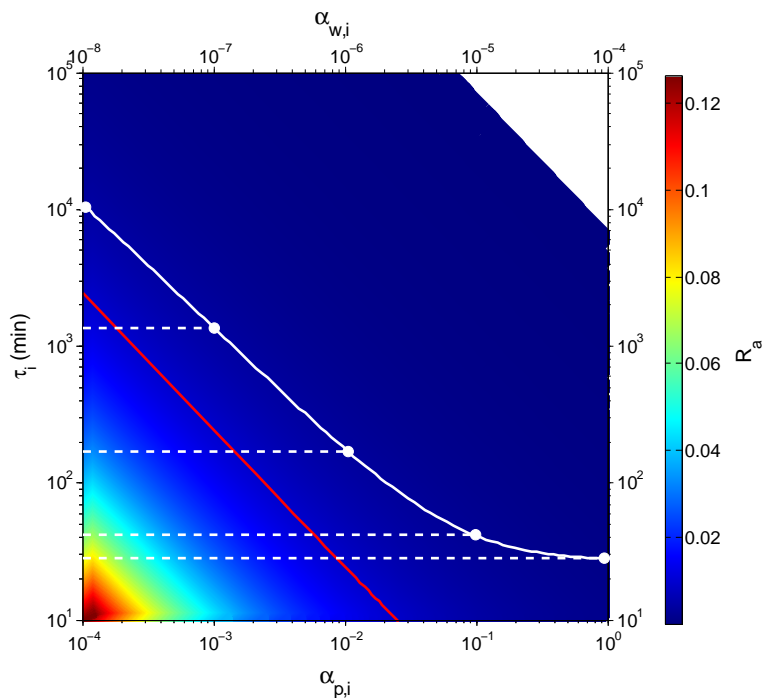


**Figure 7.** Comparison of estimated gas-particle equilibration time ( $\tau_{g/p,i}$ ) as a function of the gas-particle mass accommodation coefficient ( $\alpha_{p,i}$ , lower  $x$  axis) and the ratio of total particle surface area to the chamber wall area ( $R_a$ , colour bar), and vapor wall deposition timescale ( $\tau_{g/w,i}$ ) as a function of gas-wall mass accommodation coefficient ( $\alpha_{w,i}$ , upper  $x$  axis). White solid and dashed lines define the region where  $\tau_{g/p,i} \approx \tau_{g/w,i}$ . The red solid line represents the gas-particle equilibration time for a typical chamber experiment with seed surface area of  $\sim 1 \times 10^{-3} \mu\text{m}^2 \text{cm}^{-3}$ .

Title Page

Abstract

Introduction

Conclusions

References

Tables

Figures

◀

▶

◀

▶

Back

Close

Full Screen / Esc

Printer-friendly Version

Interactive Discussion

